

1 **Unveiling how ventilated packaging design and cold chain scenarios affect the cooling kinetics and fruit**
2 **quality for each single citrus fruit in an entire pallet**

3
4 Wentao Wu ^{1,2,3}, Paul Cronjé ⁴, Pieter Verboven ⁵, Thijs Defraeye ^{6, *}

5
6 ¹ *Chair of Building Physics, ETH Zurich, Stefano-Franscini-Platz 5, 8093 Zürich, Switzerland*

7 ² *Empa, Swiss Federal Laboratories for Materials Science and Technology, Multiscale Studies in Building*
8 *Physics, Überlandstrasse 129, 8600 Dübendorf, Switzerland*

9 ³ *Harvard Graduate School of Design, Harvard University, 20 Sumner Rd., Cambridge, 02138 MA, USA.*

10 ⁴ *Citrus Research International, Department of Horticultural Sciences, Stellenbosch University, Stellenbosch*
11 *7602, South Africa*

12 ⁵ *MeBioS, Department of Biosystems, KU Leuven, Willem de Croylaan 42, 3001 Heverlee, Belgium*

13 ⁶ *Empa, Swiss Federal Laboratories for Materials Science and Technology, Laboratory for Biomimetic*
14 *Membranes and Textiles, Lerchenfeldstrasse 5, 9014 St. Gallen, Switzerland*

15 * corresponding author, thijs.defraeye@empa.ch

16

This document is the accepted manuscript version of the following article:
Wu, W., Cronjé, P., Verboven, P., & Defraeye, T. (2019). Unveiling how ventilated packaging design and cold chain scenarios affect the cooling kinetics and fruit quality for each single citrus fruit in an entire pallet. *Food Packaging and Shelf Life*, 21, 100369 (13 pp.).
<https://doi.org/10.1016/j.fpsl.2019.100369>
This manuscript version is made available under the CC-BY-NC-ND 4.0
license <http://creativecommons.org/licenses/by-nc-nd/4.0/>

17 **Abstract**

18 Optimizing fresh fruit supply chains is essential to reduce food losses and the associated environmental
19 impact, as large amounts of energy and natural resources are embodied in these lost products. Proper
20 refrigeration of these perishable items is essential here, and the used ventilated packaging design and cold
21 chain scenario play a key role. This study pioneers in unveiling how package design, package position on a
22 pallet, package stacking pattern and cold chain scenarios affect the cooling kinetics and fruit quality evolution
23 for every single fruit of the thousands of fruit inside a pallet. This enables us to identify fruit quality
24 heterogeneities on a pallet level, where previous studies focused on an order of magnitude less fruit. For this
25 purpose, our recently developed virtual cold chain methodology is applied to these large ensembles of fruit,
26 which relies on computational fluid dynamics simulations. Of the three evaluated packaging designs for citrus
27 fruit, the Supervent package outperforms the Standard and Opentop packaging by providing the overall
28 fastest and most uniform cooling. Supervent’s performance is attributed to the alignment of ventilation
29 pathways through the lateral vent holes. The performance of the Standard package is very similar, apart from
30 the inefficient cooling at lower speeds. The Opentop packaging exhibits lengthy and non-uniform citrus fruit
31 cooling, due to the unequal distribution of the vent openings on its long and short sides, and near the top
32 surface. This unequal distribution fosters the creation of preferential pathways and faster cooling of the top
33 layer of fruit. Concerning the cold chain scenarios, forced-airflow precooling can bring down the temperature
34 the fastest after harvest. The promising scenario “ambient loading”, where citrus fruit are loaded at ambient
35 temperatures in the container, proves to be a worthy alternative. We could also show that stacking the pallet
36 in a mechanically more stable way negatively affects the cooling heterogeneity. Finally, our methodology
37 enables us to identify for a certain cold chain, which box on the pallet the customer should choose to have the
38 longest shelf life, or which box the retailer should sell first.

39

40 **Keywords**

41 virtual cold chain; citrus fruit; CFD; OpenFOAM; fruit quality; cooling

42

1. Introduction

Temperature is a key environmental parameter that affects the shelf life of fresh fruit and vegetables. A reduction of 10°C in fruit temperature typically doubles the shelf life because the product's metabolism and the associated deteriorative reactions are slowed down (Robertson, 2016; Thompson, 2004). As such, cooling of fresh produce after they are harvested, by removing the stored heat, and keeping these products cool throughout the cold chain are paramount for maximizing shelf life. Maintaining a low temperature, once the produce is cooled down, might seem trivial but is quite challenging in commercial cold chains. One reason is that the produce is usually exposed to elevated temperatures when it is transferred from one unit operation to another, for example during loading into a refrigerated container from the precooling facility. Product temperatures also rise during defrosting cycles in refrigerated containers or cold stores or during failure of the cooling system due to power outages. In addition to the initial precooling, produce thus often has to be partially re-cooled several times throughout its cold chain journey in different facilities. Fast and homogeneous (re)cooling of the fruit at different locations in each pallet of the cargo is therefore essential to minimize quality loss. By achieving an efficient cold chain: (1) food losses are reduced (Gardas, Raut, & Narkhede, 2018); (2) the spatial radius to market the produce is enlarged; (3) lengthier, but more environmentally-friendly, means of transport can be used, for example ship transport instead of airfreight; or (5) customers can keep the fruit longer fresh at home before consumption. The large impact of cooling on food losses (Arias Bustos & Moors, 2018; Gokarn & Kuthambalayan, 2017) also directly links to the environmental impact of food cold chains: for every fruit that is lost along the supply chain, the energy used in pre- and postharvest practices is indirectly lost as well (Fiore et al., 2018; Vinyes et al., 2017). Hence reducing these losses is essential for any sustainable fresh fruit industry.

The ventilated packaging in which fruit or vegetables are packed play a key role in how fast produce can be

65 (re)cooled, and how uniform this process is within, for example, a pallet of packed produce (Defraeye, Cronjé,
66 Berry, et al., 2015; Galić, Ščetar, & Kurek, 2011; Opara & Mditshwa, 2013). Ventilated cartons or plastic crates
67 are typically used for fresh produce (Opara & Mditshwa, 2013; Watkins, 2002; WPO, 2008). The cooling
68 kinetics depend on the box dimension, the total vent area, the position of the vent holes and their shape,
69 amongst others (Pathare, Opara, Vigneault, Delele, & Al-Said, 2012). Apart from the individual package design,
70 also their stacking on the pallet plays a role as often a part of the vent holes are blocked. Finally, the
71 (re)cooling efficacy of the package design is also closely related to the specific unit operation. Forced airflow
72 cooling implies horizontal airflow at high flow rates ($\sim 1 \text{ L s}^{-1} \text{ kg}^{-1}$ (Brosnan & Sun, 2001; Thompson, 2008,
73 2004)) whereas in refrigerated containers vertical airflow is present with much lower airflow rates (0.02-0.06 L
74 $\text{s}^{-1} \text{ kg}^{-1}$ (Defraeye, Cronjé, Verboven, Opara, & Nicolai, 2015)). Packaging also plays a key role in the
75 environmental impact of refrigerated supply chains. Differences in environmental impact between ventilated
76 packaging designs have been identified recently (Defraeye et al., 2016). Typical life-cycle assessment (LCA)
77 however rarely incorporates the energy and fruit quality gains from better packaging systems (Wikström,
78 Williams, Verghese, & Clune, 2014). In a recent study (Wu, Beretta, Cronje, Hellweg, & Defraeye, 2019), life-
79 cycle assessment was performed to evaluate the environmental impact of different packaging designs, where
80 significant differences were identified between ventilated carton designs. These differences in fruit quality
81 evolution between different packaging designs are expected to become particularly pronounced for very
82 perishable species (e.g. berries).

83 As packaging is so important in postharvest cold chains, a lot of valuable research was performed on the
84 relation of package design to fruit cooling (Berry, Fadiji, Defraeye, & Opara, 2017; Defraeye et al., 2013;
85 Deghannya, Ngadi, & Vigneault, 2011, 2012; Ferrua & Singh, 2009; Pathare et al., 2012). Focus areas were,
86 amongst others, the number, shape or position of vent holes, the total open area of the packaging, the impact
87 of internal packaging (plastic liners, trays) and the occurrence of airflow bypass (Thijs Defraeye, Cronjé, Berry,

88 et al., 2015). These studies relied on both experimental and simulation-based techniques. Experiments are
89 instrumental in measuring the temperature history of individual produce or airspeeds at specific positions
90 inside the ventilated cartons. Setting up such experiments is, however, quite time consuming, particularly
91 when large amounts of cartons, filled with fruit, have to be monitored. At most, only a few tens of fruit are
92 typically monitored. Computational fluid dynamics (CFD) simulations, where every individual fruit can be
93 modeled explicitly, are the preferred choice for a precise evaluation of the fruit cooling heterogeneity and
94 airflow field inside the package (Ambaw et al., 2013; Deghannya, Ngadi, & Vigneault, 2010; Norton & Sun,
95 2006; Norton, Tiwari, & Sun, 2013; Smale, Moureh, & Cortella, 2006; Wang & Sun, 2003). This explicit
96 approach avoids the need for parameterized porous media approximations but entails a high computational
97 cost. Thereby, CFD has only been applied to a single box or a few boxes of fruit, so typically for a few 100
98 fruits. The differences in airflow rates and airflow directions between the various unit operations, however,
99 require that larger entities of packages are assessed together to provide an outcome on the cooling
100 uniformity throughout the cargo. In a recent study, an entire pallet of fruit, where each fruit was explicitly
101 modeled, was evaluated for the first time with CFD for one single package design (Wu & Defraeye, 2018).
102 Clear non-uniform cooling between individual packages in each pallet was identified. As a next step, we
103 identify how package design, its positioning on a pallet, package stacking pattern but also cold chain scenario
104 affect the remaining fruit storage life of a complete pallet of fruit, and the related heterogeneities within the
105 pallet. Answering these questions will give insight in how to improve ventilated packaging designs and cold
106 chain scenarios to provide a longer and more uniform storage life of our fruit. Such comparisons between
107 packaging designs and stacking patterns on pallets are especially of interest for the postharvest industry,
108 including packhouses, precooling facility managers, exporters and importers of fresh produce but also R&D
109 researchers and container manufacturers. For this purpose, the recently developed virtual cold chain (VCC)
110 method is used (Wu et al., 2018), which relies on CFD simulations. As a case study, we target corrugated
111 fiberboard cartons filled with orange fruit, stacked on a high-cube pallet. Three packaging designs of

112 ventilated cardboard boxes are evaluated concerning cooling performance for three subsequent unit
113 operations in the refrigerated supply chain, namely forced airflow (pre)cooling, refrigerated container
114 transport and cold storage. Also, three cold chain scenarios are considered. Here, also a prediction of the
115 evolution of temperature-dependent fruit quality is included. Finally, the impact of the stacking pattern of the
116 packages on a pallet is investigated. Identifying the cooling and quality heterogeneities between individual
117 fruit on a pallet level was not done for different packaging and cold chain scenarios to our best knowledge.

119 **2. Materials and methods**

120 **2.1. *Virtual cold chain method***

121 The virtual cold chain method was developed by (Wu et al., 2018). This method is actually a CFD-based
122 workflow to obtain the thermal history as well as quality evolution of every individual fruit inside ventilated
123 packaging throughout its entire cold chain (Figure 1). In the present study, an entire pallet of fruit is targeted.
124 First, a computational model is built for a pallet for each of the unit operations (precooling, refrigerated
125 transport, cold storage). Afterward, CFD simulations, calculating airflow and heat transfer, are performed for
126 each unit operation. The thermal state of each fruit is transferred from one (virtual) unit operation (e.g.,
127 precooling) to the following one (e.g., transport) for each of the investigated cold chain scenarios. In that way,
128 the cooling behavior is simulated throughout the entire virtual cold chain. Finally, a temperature-dependent
129 kinetic rate-law is modeled to calculate the evolution of fruit quality of every single fruit, based on its
130 simulated temperature history.

131 The VCC method relies on CFD as the main pillar for estimating fruit quality evolution. This computational
132 engineering tool is commonly-used in research, R&D and industrial practice for process optimization, including

133 for making processes more green and sustainable (Azizi, Keshavarz, & Hassanzadeh, 2018; Ebrahimi-
134 moghadam, Farzaneh-gord, Arabkoohsar, & Jabari, 2018; Wu et al., 2019; Xiao, Fu, Zhu, & Zhang, 2019; Zhang
135 et al., 2018). In this study, an entire pallet of fruit is considered, where each fruit is modeled discretely with
136 CFD. This implies an exceptionally large computational effort. As such, this amount of fruit is representative
137 for industrial practice at a commercial scale, and can capture the thermal heterogeneity found in real pallets
138 of fruit.

139 **2.2. Packaging and palletization**

140 Three different package designs are evaluated, namely Standard, Supervent and Opentop (Figure 2). The
141 Standard and Supervent cartons are filled with 64 orange fruit (so 13.57 kg) and each Opentop carton is filled
142 with 60 fruit (so 12.72 kg). All fruit are placed in the carton according to a staggered pattern. The citrus fruit
143 are modeled explicitly by representing them as spheres (diameter 75 mm). The total open area (TOA) for each
144 carton is specified in Table 1.

145

146 The Standard and Supervent boxes are stacked to assemble a high-cube pallet (1.2 m x 1.0 m x 2.16 m)
147 containing 80 cartons and holding 5120 fruit (Figure 3). In total, 8 layers are stacked regularly on top of one
148 another, where each layer contains 10 cartons. In total, 3 rows are present (Row1, Row2 and Row3) along the
149 horizontal flow path for precooling and cold storage, and 8 layers (L1-L8) are present along the vertical flow
150 path for refrigerated container transport. Each layer contains 10 cartons (C01-C10). For each layer, Row1 and
151 Row2, respectively, have 3 cartons, whereas Row3 has 4 cartons (Figure 3).

152

153 For the Opentop boxes, 65 cartons are stacked to assemble a high-cube pallet (1.2 m x 1.0 m x 2.21 m) (Figure
154 3), which holds 3900 fruit. In total, 13 layers are stacked regularly on top of one another, and each layer

155 contains 5 cartons. This results in 2-3 rows (Row1, Row2 and Row3) along the horizontal flow pathway for
156 precooling and cold storage, and 13 layers (L1-L13) along the vertical flow pathway for refrigerated container
157 transport. Each layer contains 5 cartons (C01-C05). Note that Opentop cartons are precooled with airflow
158 perpendicular to their short side (1 m wide) of the pallet (1 x 1.2 m), whereas Standard and Supervent cartons
159 are precooled with airflow perpendicular to their long side (1.2 m wide). The main reason is that this helps to
160 counteract for the reduced fruit stacking density for Opentop packaging. This reduced density implies that less
161 fruit can be packed in the same pallet volume, due to their less dense stacking in the Opentop package. By
162 positioning and cooling the pallet along its short side in the precooler, more Opentop pallets can be placed in
163 one precooling room, so a larger amount of fruit can be cooled simultaneously. Even in this case, the resulting
164 stacking density for a single pallet is lower than for Supervent.

165 In addition to the regular 8-layers stacking of the Supervent cartons, staggered stacking is also evaluated
166 (Figure 4) as this can provide additional stability of the pallet. This configuration however blocks a part of the
167 vertical vent holes and thereby some of the vertical ventilation pathways. By comparing both stacking
168 patterns, we aim to evaluate how the cooling rate is affected by this more stable alternative.

169 **2.3. Computational model**

170 The cold chain involves three different unit operations, namely precooling, refrigerated transport and cold
171 storage. As such, three separate computational models (Figure 5) are constructed. For precooling and
172 refrigerated storage, air ventilates the pallet horizontally (Figure 5a), whereas for refrigerated container
173 transport, air ventilates the pallet vertically (Figure 5b). The inlet and outlet sections are chosen long enough
174 to avoid an impact of these boundary conditions on the airflow and heat transfer in the pallet. **The length of
175 the inlet and outlet section is 0.4 m and 1.6 m, respectively.** The inlet and outlet could be located relatively
176 close to the pallet because a large pressure drop is created over the pallet. To avoid highly skewed grid cells
177 (control volumes) near the point of contact between two fruit during mesh generation, a gap of about 3 mm is

178 left between adjacent fruit. This was found to lead to the most stable numerical solution, whereas point
179 contact or small overlaps between the fruit provided unstable solutions in some cases.

180 Meshing of the computational models was done using tetrahedral cells with about 40 million tetrahedral cells
181 for each model. Tetrahedral control volumes are placed on the inside and outside surfaces of the fruit. The
182 wall y^+ is smaller than 185, 6 and 3 for precooling, refrigerated transport and cold storage, respectively. The
183 spatial discretization error was quantified via a mesh dependency study combined with Richardson
184 extrapolation. It is 2.5% for mass flow rates in the box and 5% for convective heat transfer coefficients on the
185 fruit surface.

186 On the outlet, the imposed airflow rate is a uniform air speed. Its value depends on the specific cold chain unit
187 operation. The airflow rates (see Table 2) in the present study are 0.2, 0.02 and 0.002 L s⁻¹ kg⁻¹ of fruit for
188 precooling, transport and storage. These flow rates are chosen to be representative of the current commercial
189 practice. Note that these flow rates differ a factor 10 from one another. Note that this implies that for the
190 Opentop packaging, which has a lower packing density per pallet (3900 fruit instead of 5120 for Standard and
191 Supervent), the speed is slightly lower than for the other packaging (Table 2). This effect is counteracted in
192 part by the fact that Opentop pallets are cooled along their short side, in comparison to Standard and
193 Supervent pallets. This, in turn, reduces the total inlet surface area which increases the speed for a certain
194 flow rate. At the inlet, the atmospheric pressure is imposed with a low turbulence intensity of 0.1%. The air
195 temperature at the inlet, or the so-called delivery-air temperature, is different for each evaluated supply chain
196 scenarios (see Table 2).

197 The lateral boundaries of the extended inlet and outlet sections and the vent openings on the lateral carton
198 surfaces of the complete pallet are specified as a symmetry boundary condition. This choice assumes that
199 every single pallet has another adjacent pallet. This idealized assumption does not account for possible gaps

200 between the pallets, which can be present in reality. The impact of such gaps was investigated by numerical
201 simulations recently (Defraeye, Cronjé, Verboven, Opara, & Nicolai, 2015). Although such gaps are blocked as
202 much as possible with void plugs in practice, they can still be present sometimes, and can form preferential
203 pathways between pallets. The size and location of such gaps are however very difficult to predict or quantify
204 and can differ between different shipments. In this study, the impact of possible gaps between pallets was not
205 included as a design parameter. No-slip surfaces with zero roughness are used for carton surfaces and fruit
206 surfaces.

208 **2.4. Numerical simulation**

210 The simulations are performed with the open source CFD code OpenFOAM 2.4.0. The Reynolds-averaged
211 Navier-Stokes (RANS) equations with the shear-stress transport $k-\omega$ turbulence model (Menter, 1994) are
212 used to solve for turbulent flow. A turbulence model was used since even at low speeds, high airspeeds, so
213 turbulent flow, can occur near the vent holes. Wall functions are applied to solve airflow and heat exchange in
214 the boundary layer near the fruit and carton surfaces. The applied wall functions switch automatically from a
215 standard wall function approach to a low-Reynolds number formulation, based on the grid density in the
216 boundary layer. This switching takes place around a y^+ value of 11, using a blending function between the
217 viscous and logarithmic region. In this way, the wall functions have a wide range of y^+ values in which they are
218 applicable, and can be accurately used for both low- and high-Reynolds number turbulent flows. The accuracy
219 of the shear-stress transport turbulence model combined with wall functions to model the boundary layer
220 was validated already by the authors and co-workers on several occasions (Ambaw et al., 2012; Defraeye et
221 al., 2013; Delele et al., 2009) for the same turbulence model and a similar geometrical model as used in the
222 present study. All the details of the validation procedures can be found there. The agreement between CFD

223 and experiments was satisfactory. As an example, for Supervent packages, the differences in seven-eighths
224 cooling time were below 5%. The initial temperature of cartons and the fruit was 21 °C. The thermal
225 properties of the fruit are a density of 960 kg m^{-3} , thermal conductivity of $0.386 \text{ W m}^{-1}\text{K}^{-1}$ and specific heat
226 capacity of $3850 \text{ J kg}^{-1}\text{K}^{-1}$ (Wu et al., 2018; Wu & Defraeye, 2018). A time step of 60 s was used, as determined
227 from a sensitivity analysis. First, the steady airflow field is calculated for every unit operation. In the next step,
228 the transient heat conservation equation is solved in the air and fruit domain. Thereby, the air and fruit
229 temperature profiles are obtained throughout the complete cold chain. As the airflow was steady over time
230 (as no buoyancy was modeled), the airflow field did not need to be recomputed anymore during the transient
231 simulations. This removed the need for solving the airflow conservation equations during the transient cooling
232 process. As such, the computational cost was reduced a lot (Wu et al., 2018; Wu & Defraeye, 2018). The two-
233 step approach is often applied for forced-air cooling applications.

234 Not accounting for buoyancy essentially means that no temperature-driven density difference flow is
235 modeled, so only forced-convective flow is considered. In addition, this implies that the temperature does not
236 influence the flow field, by which heat can be considered as a passive scalar. As mentioned, this assumption
237 simplifies the solution procedure a lot and reduces the computational cost. Especially at very lower airspeeds,
238 such as in storage rooms, and at the start of the cooling process, when temperature differences in the air are
239 larger, buoyancy could however contribute. Investigating the impact of buoyancy in such cases is definitely a
240 topic of further research, but will pose challenges to numerical stability, convergence and computational cost.
241 For this reason, it is very rarely taken into account in CFD studies in postharvest engineering.

242 The advection terms are discretized by the second-order upwind scheme. The time derivative is discretized by
243 the first-order, bounded, implicit Euler scheme. The SIMPLE algorithm and merged PISO-SIMPLE (PIMPLE)
244 algorithm are adopted for velocity-pressure coupling for steady state and transient simulations, respectively.
245 Further details on the numerical modeling approach, model assumptions, solution method and discretization

246 approach can be found in (Wu et al., 2018; Wu & Defraeye, 2018), including on the other physics that are
247 included.

248

249 **2.5. Kinetic rate-law quality model**

250 A kinetic rate-law model for fruit quality evolution was presented previously (Wu et al., 2018; Wu & Defraeye,
251 2018), so only the main aspects are highlighted here. This simple model quantifies the change in overall fruit
252 quality, indicated by parameter A , based on a kinetic rate law (Robertson, 2016; Van Boekel, 2008):

$$-\frac{dA}{dt} = kA^n \quad (1)$$

253 with t the time [s], k the rate constant [s^{-1}], n the order of a reaction. We assume a zero-order reaction here
254 for the change of the overall quality A . This means that the temporal change of A for a specified temperature
255 is a line, where the slope is linked to the magnitude of k . An example of a zero-order reaction is enzymatic
256 degradation (Robertson, 2016; Van Boekel, 2008). First-order reaction (such as vitamin loss), can also be
257 modeled similarly.

258 The rate constant k quantifies the temperature relationship of the fruit quality loss (Robertson, 1993):

$$k(T) = k_0 e^{\frac{-E_a}{RT}} \quad (2)$$

259 where k_0 is a constant [d^{-1}], E_a is the activation energy [$J \text{ mol}^{-1}$], R is the ideal gas constant ($8.314 \text{ J mol}^{-1} \text{ K}^{-1}$), T
260 is the absolute temperature [K]. The constant k_0 and E_a are inferred from quality decay data.

261 This model was calibrated based on following assumptions, stemming from experimental data: citrus fruit can
262 be stored for approximately 56 d at 4 °C (Cantwell, 2001) where a rise in temperature of 10 °C from a certain
263 temperature halves the storage life. As such, if the fruit is kept 56 d hours at 4 °C, the entire quality, and

264 thereby also the fruit, is assumed to be lost, so $A(56 \text{ d}, 4 \text{ }^\circ\text{C}) = 0\%$. As such, E_a and k_0 were determined to be
265 $4.59 \times 10^4 \text{ J mol}^{-1}$ and $7.89 \times 10^6 \text{ d}^{-1}$, respectively. After calibrating this quality model, the temperature-
266 dependent evolution of this fruit quality of every single fruit was predicted throughout the cold supply chain.
267 The temperature used to calculate the quality evolution can be for example the core temperature or the
268 average fruit temperature. In this study, the fruit core temperature was used to derive the quality evolution of
269 every single fruit. This choice is conservative as the fruit core is typically the last location that reaches the
270 target temperature.

271

272 **2.6. Different cold chains**

273 Three cold chain scenarios (see Table 2) are assessed for their impact on the cooling of a pallet of fruit. These
274 are currently employed as postharvest supply chain strategies in the citrus fruit industry in South Africa.

275 The “forced-airflow precooling” chain includes cooling (3 d to 3 °C), refrigerated transport at cold-
276 disinfestation temperatures for pests (24 d to -1 °C) and subsequent cold storage (14 d to 4 °C). This chain
277 implies rapid removal of the bulk of the stored heat by precooling, followed by further removal during
278 refrigerated transport. The next cold chain “ambient cooling” does not include forced-airflow cooling.

279 Alternatively, fruit are kept in standard cold storage for 5 d to 3 °C, before shipment, so slow cooling. This
280 strategy is often named static cooling in the citrus industry. Following that, fruit are loaded in a refrigerated
281 container for transport (24 d to -1 °C) and subsequent cold storage (14 d to 4 °C) after shipment. In the third
282 cold chain, “ambient loading” (Defraeye, Verboven, Opara, Nicolai, & Cronjé, 2015), fruit are loaded directly
283 into the container after packaging. Following 24 d at -1 °C, fruit are stored for 14 d in 4 °C. Ambient loading is
284 applied in South Africa to reduce the cold chain length and to enable cooling after harvest in areas where
285 there are insufficient facilities to precool.

286 **2.7. Evaluation of cooling rate**

287 The fruit's cooling rate is quantified by its temperature-time history. This is measured in the center core of
288 each citrus fruit. From these core temperature profiles (T [K]) the dimensionless temperature change (Y) was
289 calculated.

$$Y = \frac{T - T_a}{T_i - T_a} \quad (3)$$

290 where subscripts i and a imply the initial fruit temperature and the air's delivery temperature in the cold chain
291 unit operations, respectively. From Y , the seven-eighths cooling (or heating) time (SECT, $t_{7/8}$) was calculated.
292 The $t_{7/8}$ is the time required to bring the temperature difference between initial-fruit and delivery-air
293 temperature down by seven eighths ($Y=0.125$). The SECT is a useful parameter to characterize the cooling
294 behavior of the fruit in each of the unit operations.

295

296 **3. Results and discussion**

297 **3.1. Cooling kinetics of individual unit operations**

298 The cooling behavior is evaluated separately for each unit operation to quantify how large the differences
299 between the three package designs are. The fruit core temperature is used here for calculating the SECT of
300 every single fruit. The reason is that the core temperature is typically the last location that reaches the target
301 temperature. For this reason, it is measured in commercial cooling operations, and especially in cold
302 treatment protocols, for monitoring the cooling process by inserting a temperature point probe. The use of
303 this temperature to assess fruit cooling is thereby the most conservative scenario.

304 In Figure 6, the SECT is depicted for all unit operations and packaging by showing the average value and

305 standard deviation over all fruit in the pallet. Here, all fruit are cooled down completely to the delivery-air
306 temperature within one unit operation. These SECT data of all the fruit in the pallet are also presented in
307 Figure 7, but now grouped and averaged per vertical column for each separate carton (C01-C10, for
308 precooling and storage so horizontal airflow) or per horizontal layer (L1-L13) (for transport so vertical airflow).
309 Next, to the average values per column and layer, the standard deviations are also shown. In Figure 8, the
310 SECT per box is represented for all unit operations and packaging.

311

312

313 **Precooling**

314 The Standard and Supervent packaging cool similar, which is in agreement with previous studies of the
315 authors for a smaller computational model, with a slightly different computational model build-up (Defraeye
316 et al., 2014). At the currently evaluated flow rates ($0.2 \text{ L s}^{-1} \text{ kg}^{-1}$), the Standard packaging cools slightly faster,
317 when averaged over the pallet. For both packagings, the more upstream the box is, the faster it cools,
318 although the flow rates through each row of boxes is the same due to the conservation of mass, i.e. all air
319 which enters the pallet also leaves. One reason is that the downstream boxes are exposed to higher air
320 temperatures as heat is added to the flow from the fruit upstream, by which the fruit more downstream will
321 cool slower. This principle is also valid for other packaging and other unit operations. Also, the blockage of the
322 vent holes for Standard and Supervent packages induces a high SECT for cartons C08 and C09, which are
323 double or triple than those of the upstream boxes (C01-C03).

324 The Opentop packaging cools slower and also more heterogeneously than the other two. This is counter-
325 intuitive at first as Opentop cartons have the largest open area of vent openings on both its long and short
326 side of the packaging (Table 1). This is due to:

- 327 • The difference in TOA between the long and short side of the package. First, this creates a difference in
328 aerodynamic resistances, by which the preferential pathway will be through C03-C05 instead of C01-
329 C02, leading to higher speeds there, which can be seen from Figure 9b. Also, the cooling air accesses
330 more easily most of the fruit in C03-C05 since the ventilation opening is wider. An additional reason is
331 that the path length for airflow is longer for C01. As such, the air is heated up more at the point when
332 it reaches the fruits at the back of the package, by which fruit cooling in these packages is slowed
333 down.
- 334 • The configuration of the vent openings on the short and long sides of each box. Since they are not
335 distributed that homogeneously compared to the other two packages, but mainly have large openings
336 at the top, the cooling air is directed primarily over the top layer of fruit. As such, the access of the air
337 to the bottom layer of fruit in each box is more difficult. As such, this bottom layer was also found to
338 cool slower than the top layer, inducing an additional cooling heterogeneity. On average, the bottom
339 layer cooled less than 5% slower than the top layer (based on the SECT). However, individual
340 differences in SECT of over 50% are found between fruit in the bottom and top layer.
- 341 • The airflow rate ($0.2 \text{ L s}^{-1} \text{ kg}^{-1}$) results in a slightly lower speed in the Opentop packaging, due to the
342 lower packing density (Table 2). Also, the maximal speeds (Figure 9) are lower as less flow acceleration
343 occurs near the vent openings, due to the large total open area (Table 1).

344 Although no blockage of vent openings is present with the Opentop packaging, some upstream boxes still cool
345 more than twice as fast as the downstream ones. This limited performance of the Opentop packaging
346 contradicts the experimental study of (Wu, Haller, Cronje, & Defraeye, 2018), which found a better
347 performance for the Opentop packaging for precooling. There are several reasons that can be attributed for
348 these differences. The experiments were conducted on a commercial precooling facility. As such, the airflow
349 rate through the different packages could not be controlled, as this was the result of the cooling infrastructure

350 and the pressure resistance of the pallets. As such the airflow rates differed for Supervent and Opentop. In
351 the current computational study, similar airflow rates were imposed for both Supervent and Opentop. This
352 makes a comparison between both studies difficult. The computational study shows however that at a similar
353 airflow rate, the Supervent packaging seems to cool better than Opentop packaging. Also, note that the fruit
354 size and packing density differed in both studies. **Refrigerated transport**

355 The Supervent packaging cools faster than the other two packagings. This is mainly attributed to the specific
356 vent hole configuration, where vent openings are positioned along the side edges of the packaging. As such,
357 vertical ventilation channels of cold air are formed, which can be seen from Figure 9a. Combined with the
358 central opening at the bottom and top, a very uniform distribution of the cooling air through the package is
359 achieved. Opentop packaging has very small ventilation openings by which locally very high speeds are
360 generated, which can be seen from Figure 9a. The access of the cold air to the rest of the fruit is limited and
361 also the airflow distribution is much less uniform. All packages cool progressively slower towards the top of
362 the pallet, and this occurs in a quite linear manner.

363 **Cold storage**

364 The Supervent packaging cools faster than the other two packagings. A lot of similar observations can be
365 made as for precooling, for example, the SECT distribution between the different boxes. The main reason is
366 that the airflow direction is the same, but only the airflow rate differs. At low airflow rates (cold storage) the
367 fruit have a less uniform temperature reduction than at high airflow rates (precooling) for Standard and
368 Supervent, but this is not found for Opentop which cools similarly uniform (but not similarly fast) in both unit
369 operations. The Standard packaging however cools much slower than the other two, where for precooling it
370 cooled the fastest. This is an interesting observation, particularly since the Opentop pallet contains 24 % less
371 fruit, and is subjected to slightly lower airspeed.

372 A first reason to explain this observation is that at different airspeeds, a different velocity distribution is found
373 in the pallet for each packaging, which can be seen from the streamlines for precooling and storage for
374 Opentop (Figure 9). This will thereby also induce a difference in the cooling of the individual fruit in the
375 packaging for the different unit operations. For Opentop, for example the cold airflow penetrates the stacked
376 fruit inside the packaging better at low airspeeds, which induces better access of the cooling air to the bottom
377 layer of fruit. This reduces the heterogeneity between the bottom and top layer of fruit. At high speeds
378 (precooling) on the other hand, the fast flowing horizontal air only accesses the top fruit and does not cool the
379 lower fruit on the bottom layers. As such, Opentop packaging seems to cool the two layers more efficiently, in
380 a relative way, at lower air speeds.

381 A second reason is that at lower airspeeds, the air is able to extract more heat (relatively) as it passes over the
382 fruit in the first packages (e.g. C01-C03), after which the air temperature also rises more during cold storage
383 when passing the different boxes. As such, for cold storage, the boxes more downstream on the pallet will
384 cool (relatively) slower than those upstream, compared to forced-air cooling. This increased heterogeneity for
385 cold storage, compared to precooling, can clearly be seen in Figure 8, and is especially pronounced for the
386 Standard package. As a third reason, the cartons C08 and C09 seem to cool even slower during storage, which
387 could indicate that the cooling air penetrates these two boxes at even further reduced airspeeds.

388

389 **Summary**

390 Throughout all unit operations, Supervent outperforms the other packages, by which it can be considered the
391 fastest and most uniformly cooling package. This is attributed to the specific vent hole configuration, where
392 the vent holes are positioned along the side edges of the packaging. This enables the vent holes to form
393 ventilation channels of cold air for both vertical and horizontal flow. The superior performance of Supervent

394 was identified before, but for smaller entities of fruit (Defraeye, Cronjé, Verboven, et al., 2015; Defraeye et
395 al., 2013). For all boxes, the spatial heterogeneity in cooling behavior inside the pallet is very apparent for
396 different unit operations, where precooling provides the most uniform cooling. This heterogeneity will directly
397 affect fruit quality and shelf life as well, as illustrated in the next section. It needs to be mentioned that all
398 packages were evaluated at similar airflow rates (Table 2). In reality, the resistance to airflow of the palletized
399 package and the resulting pressure drop over the pallet will also determine the resulting air speed (Defraeye
400 et al., 2014).

402 ***3.2. Cooling kinetics and quality evolution of complete cold chain scenarios***

403 By combining subsequent unit operations into a cold chain, three different cold chain scenarios are simulated
404 (Table 2). In Figure 10, their thermal history is given for all packaging designs, as presented by the volume-
405 averaged temperature of all fruit inside the pallet. This implies as well that the volume-averaged temperature
406 of each fruit is used, so averaging is not done based on core temperature. It is clear that the forced-airflow
407 precooling scenario provides the fastest cooling. Ambient cooling (static cooling) only reduces the fruit
408 temperature very slowly, by which the fruit still did not reach the set point temperature at the time of loading
409 into the refrigerated container for transport. The differences between the packages are relatively limited, but
410 show an inferior performance for the Opentop packages.

411
412
413
414 Using this thermal history, the quality evolution of the fruit in the pallet is calculated for several cold chain

415 scenarios for each packaging design. The fruit core temperature is used to derive the quality evolution of
416 every single fruit. In Figure 11, the evolution in the quality of every single fruit in two different boxes (shown
417 in Figure 3) is shown for the three package designs and the three scenarios. The remaining end quality is given
418 as the percentage of initial quality ($A_{ini}=100\%$), and the fruit is considered lost if all quality is gone ($A_{end}=0\%$).
419 These two different boxes are chosen in that way that they are exposed to the most extreme (high and low)
420 approach flow air temperatures. To this end, one box (Box03) is always located upstream, so at the cold air
421 inflow side, and one box is located downstream (Box 62 for Opentop and Box 79 for the other two packages)
422 for precooling, transport and storage. The aim is to improve the quantification of the heterogeneity in the
423 quality evolution within a pallet, which originated from the temperature heterogeneity (Figure 8).

424 The forced-airflow precooling and ambient loading cold chain have a quite homogeneous quality evolution.
425 On average over the entire pallet (results not reported), very similar values are found, despite the clear
426 differences in cooling behavior (Figure 10). The rather limited differences between the two protocols are
427 attributed to the timescales for fruit quality decay, which are much larger than those for cooling. As such, a
428 faster cooling via precooling in the first few days, compared to cooling inside the container, does not lead to
429 significant differences in the quality loss, which occurs much slower. Note however that since the ambient
430 loading scenario has a shorter duration, its end quality is even higher than for the forced-airflow precooling
431 chain. The logistical advantage of saving time before shipment by ambient loading takes the upper hand over
432 cooling faster. Note that the quality variation within the pallet (box 03 vs. box 79 or 62) is however larger for
433 ambient loading. The ambient cooling chain, on the other hand, induces a much larger quality loss. This is
434 directly linked to the prolonged storage with much slower cooling rates, and the resulting more elevated fruit
435 temperatures before shipment. The differences between packaging designs are quite limited, which is again
436 related to the different timescales in cooling and quality decay. Opentop exhibits a slightly lower quality as it
437 had the overall worst cooling behavior over most unit operations (Figure 6).

438

439 **3.3. Cooling kinetics of different stacking patterns**

440 The impact of the stacking pattern (Figure 4) on the cooling kinetics is evaluated in Figure 12. The averaged
441 seven-eighths cooling time for each box, scaled with the average SECT for that pallet for that unit operation,
442 namely $SECT_{avg}$, is shown for the Supervent packaging for three unit operations for regular and staggered
443 stacking. The stacking pattern significantly affects the cooling heterogeneity within the pallet for each unit
444 operation. As expected, for vertical airflow, this leads to a higher heterogeneity within the pallet (vertical
445 direction) but also within a certain layer of boxes. In addition, for precooling and storage, the staggered
446 stacking leads to a very inefficient cooling of the boxes C08 and C09 in the bottom layer. In stacking cartons
447 on a pallet, there will be a tradeoff between mechanical stability and achieving uniform cooling of the pallet
448 throughout the cold chain. As such, apart from the individual package design, their pallet stacking plays a role
449 concerning vent-hole blockage.

450

451

452

4. Conclusions

This pioneering study unveiled how ventilated packaging design and cold chain scenarios affect the cooling kinetics and fruit quality evolution for each of the thousands of fruit packed inside a pallet. Concerning the three evaluated packaging designs, the Supervent package outperformed the others by providing overall the fastest and most uniform (homogeneous) cooling. This is attributed to the formation of aligned ventilation pathways via the lateral vent holes. The performance of the Standard package was very similar during forced airflow cooling, but at lower speeds, more inefficient cooling was observed. The Opentop packaging exhibited rather high and non-uniform fruit cooling times. The main causes were the unequal distribution of the vent openings on the long and short sides, creating preferential pathways, and the fact that these openings were located at the top of the package, so inducing preferential cooling of the top layer of fruit. Concerning the cold chain scenarios, forced-airflow precooling was able to bring down the fruit pulp temperature the fastest after harvest. Ambient loading, where “warm” fruit are loaded at ambient temperatures in the container, proved to be a promising alternative. Despite its slightly slower cooling, it provides a logistical advantage of saving time by direct loading the cargo in the container. This shorter cold chain also resulted in a higher final product quality. The ambient cooling scenario, where fruit are stored in a cold store before loading in the container, is not advised as it induces much higher quality losses. Finally it was shown that the stacking of the pallet in a mechanically more stable way negatively affected the cooling heterogeneity, due to blockage of the vent holes.

By applying our recently developed virtual cold chain methodology for such large ensembles of fruit, we could obtain essential insights, which were not visible before on smaller computational models. We were able, amongst others, to identify for a certain cold chain, which specific box on the pallet the customer should choose to have the longest shelf life, or also which box the retailer should sell first. Such results can be very

475 useful for logistics planning as well.

476 Finally, the obtained data on cooling and quality evolution of individual fruit, and the role of packaging, can be
477 incorporated in life-cycle assessment. Thereby, data gaps in LCA can be closed successfully by providing more
478 accurate data on cold-chain energy use for fruit, compared to what is available, for multiple packaging
479 options.

480 **5. Acknowledgments**

481 The authors acknowledge the Coop Research Program of the ETH Zurich World Food System Center and the
482 ETH Foundation for supporting this project. We also acknowledge the support of the Swiss National Science
483 Foundation SNSF (project 200021_169372).

484

485

6. References

- Ambaw, A., Delele, M. A., Defraeye, T., Ho, Q. T., Opara, L. U., Nicolai, B. M., & Verboven, P. (2013). The use of CFD to characterize and design post-harvest storage facilities: Past, present and future. *Computers and Electronics in Agriculture*, *93*, 184–194. <https://doi.org/10.1016/j.compag.2012.05.009>
- Ambaw, Alemayehu, Verboven, P., Delele, M. a., Defraeye, T., Tijssens, E., Schenk, A., & Nicolai, B. M. (2012). CFD Modelling of the 3D Spatial and Temporal Distribution of 1-methylcyclopropene in a Fruit Storage Container. *Food and Bioprocess Technology*, *6*(9), 2235–2250. <https://doi.org/10.1007/s11947-012-0913-7>
- Arias Bustos, C., & Moors, E. H. M. (2018). Reducing post-harvest food losses through innovative collaboration: Insights from the Colombian and Mexican avocado supply chains. *Journal of Cleaner Production*, *199*, 1020–1034. <https://doi.org/10.1016/j.jclepro.2018.06.187>
- Azizi, K., Keshavarz, M., & Hassanzadeh, H. (2018). Consideration of inclined mixers embedded inside a photobioreactor for microalgae cultivation using computational fluid dynamic and particle image velocimetry measurement. *Journal of Cleaner Production*, *195*, 753–764. <https://doi.org/10.1016/j.jclepro.2018.05.253>
- Berry, T. M., Fadiji, T. S., Defraeye, T., & Opara, U. L. (2017). The role of horticultural carton vent hole design on cooling efficiency and compression strength: A multi-parameter approach. *Postharvest Biology and Technology*, *124*, 62–74. <https://doi.org/10.1016/j.postharvbio.2016.10.005>
- Brosnan, T., & Sun, D. W. (2001). Precooling techniques and applications for horticultural products - a review. *International Journal of Refrigeration*, *24*, 154–170. Retrieved from <http://www.sciencedirect.com/science/article/pii/S0140700700000177>

- 507 Cantwell, M. (2001). *Properties and recommended conditions for long-term storage of fresh fruits and*
508 *vegetables.*
- 509 Defraeye, T., Cronjé, P., Verboven, P., Opara, U. L., & Nicolai, B. (2015). Exploring ambient loading of citrus
510 fruit into reefer containers for cooling during marine transport using computational fluid dynamics.
511 *Postharvest Biology and Technology, 108*, 91–101. <https://doi.org/10.1016/j.postharvbio.2015.06.004>
- 512 Defraeye, T., Lambrecht, R., Delele, M. A., Tsige, A. A., Opara, U. L., Cronjé, P., ... Nicolai, B. (2014). Forced-
513 convective cooling of citrus fruit: Cooling conditions and energy consumption in relation to package
514 design. *Journal of Food Engineering, 121*(1). <https://doi.org/10.1016/j.jfoodeng.2013.08.021>
- 515 Defraeye, T., Verboven, P., Opara, U. L., Nicolai, B., & Cronjé, P. (2015). Feasibility of ambient loading of citrus
516 fruit into refrigerated containers for cooling during marine transport. *Biosystems Engineering, 134*, 20–
517 30. <https://doi.org/10.1016/j.biosystemseng.2015.03.012>
- 518 Defraeye, Thijs, Cronjé, P., Berry, T., Opara, U. L., East, A., Hertog, M., ... Nicolai, B. (2015). Towards integrated
519 performance evaluation of future packaging for fresh produce in the cold chain. *Trends in Food Science*
520 *and Technology, 44*(2), 201–225. <https://doi.org/10.1016/j.tifs.2015.04.008>
- 521 Defraeye, Thijs, Cronjé, P., Verboven, P., Opara, U. L. U. L., & Nicolai, B. (2015). Exploring ambient loading of
522 citrus fruit into reefer containers for cooling during marine transport using computational fluid dynamics.
523 *Postharvest Biology and Technology, 108*, 91–101. <https://doi.org/10.1016/j.postharvbio.2015.06.004>
- 524 Defraeye, Thijs, Lambrecht, R., Delele, M. A., Tsige, A. A., Opara, U. L., Cronjé, P., ... Nicolai, B. (2014). Forced-
525 convective cooling of citrus fruit: Cooling conditions and energy consumption in relation to package
526 design. *Journal of Food Engineering, 121*(1), 118–127. <https://doi.org/10.1016/j.jfoodeng.2013.08.021>
- 527 Defraeye, Thijs, Lambrecht, R., Tsige, A. A., Delele, M. A., Opara, U. L., Cronjé, P., ... Nicolai, B. (2013). Forced-

528 convective cooling of citrus fruit: Package design. *Journal of Food Engineering*, 118(1), 8–18.
529 <https://doi.org/10.1016/j.jfoodeng.2013.03.026>

530 Defraeye, Thijs, Nicolai, B., Kirkman, W., Moore, S., Niekerk, S. V. S. van, Verboven, P., & Cronjé, P. (2016).
531 Integral performance evaluation of the fresh-produce cold chain: A case study for ambient loading of
532 citrus in refrigerated containers. *Postharvest Biology and Technology*, 112, 1–13.
533 <https://doi.org/10.1016/j.postharvbio.2015.09.033>

534 Dehghannya, J., Ngadi, M., & Vigneault, C. (2010). Mathematical modeling procedures for airflow, heat and
535 mass transfer during forced convection cooling of produce: A review. *Food Engineering Reviews*, 2(4),
536 227–243. <https://doi.org/10.1007/s12393-010-9027-z>

537 Dehghannya, J., Ngadi, M., & Vigneault, C. (2011). Mathematical modeling of airflow and heat transfer during
538 forced convection cooling of produce considering various package vent areas. *Food Control*, 22(8), 1393–
539 1399. <https://doi.org/10.1016/j.foodcont.2011.02.019>

540 Dehghannya, J., Ngadi, M., & Vigneault, C. (2012). Transport phenomena modelling during produce cooling for
541 optimal package design: Thermal sensitivity analysis. *Biosystems Engineering*, 111(3), 315–324.
542 <https://doi.org/10.1016/j.biosystemseng.2012.01.001>

543 Delele, M. A., Schenk, A., Tijskens, E., Ramon, H., Nicolaï, B. M., & Verboven, P. (2009). Optimization of the
544 humidification of cold stores by pressurized water atomizers based on a multiscale CFD model. *Journal of*
545 *Food Engineering*, 91(2), 228–239. <https://doi.org/10.1016/j.jfoodeng.2008.08.027>

546 Ebrahimi-moghadam, A., Farzaneh-gord, M., Arabkoohsar, A., & Jabari, A. (2018). CFD analysis of natural gas
547 emission from damaged pipelines : Correlation development for leakage estimation. *Journal of Cleaner*
548 *Production*, 199, 257–271. <https://doi.org/10.1016/j.jclepro.2018.07.127>

- 549 Ferrua, M. J., & Singh, R. P. (2009). Modeling the forced-air cooling process of fresh strawberry packages, Part
550 III: Experimental validation of the energy model. *International Journal of Refrigeration*, 32(2), 359–368.
551 <https://doi.org/10.1016/j.ijrefrig.2008.04.011>
- 552 Fiore, A., Lardo, E., Montanaro, G., Laterza, D., Loiudice, C., Berloco, T., ... Xiloyannis, C. (2018). Mitigation of
553 global warming impact of fresh fruit production through climate smart management. *Journal of Cleaner
554 Production*, 172, 3634–3643. <https://doi.org/10.1016/j.jclepro.2017.08.062>
- 555 Galić, K., Ščetar, M., & Kurek, M. (2011). The benefits of processing and packaging. *Trends in Food Science and
556 Technology*, 22(2–3), 127–137. <https://doi.org/10.1016/j.tifs.2010.04.001>
- 557 Gardas, B. B., Raut, R. D., & Narkhede, B. (2018). Evaluating critical causal factors for post-harvest losses (PHL)
558 in the fruit and vegetables supply chain in India using the DEMATEL approach. *Journal of Cleaner
559 Production*, 199, 47–61. <https://doi.org/10.1016/j.jclepro.2018.07.153>
- 560 Gokarn, S., & Kuthambalayan, T. S. (2017). Analysis of challenges inhibiting the reduction of waste in food
561 supply chain. *Journal of Cleaner Production*, 168, 595–604. <https://doi.org/10.1016/j.jclepro.2017.09.028>
- 562 Menter, F. R. (1994). Two-Equation Eddy-Viscosity Turbulence Models for Engineering Applications. *AIAA
563 Journal*, 32(8), 1598–1605. <https://doi.org/10.2514/3.12149>
- 564 Norton, T., & Sun, D.-W. (2006). Computational fluid dynamics (CFD) - an effective and efficient design and
565 analysis tool for the food industry: A review. *Trends in Food Science and Technology*, 17(11), 600–620.
566 <https://doi.org/10.1016/j.tifs.2006.05.004>
- 567 Norton, T., Tiwari, B., & Sun, D. W. (2013). Computational fluid dynamics in the design and analysis of thermal
568 processes: a review of recent advances. *Critical Reviews in Food Science and Nutrition*, 53(3), 251–275.
569 <https://doi.org/10.1080/10408398.2010.518256>

570 Opara, U. L., & Mditshwa, A. (2013). African Journal of Agricultural Research A review on the role of packaging
571 in securing food system: Adding value to food products and reducing losses and waste. *African Journal of*
572 *Agricultural Research*, 8(22), 2621–2630. <https://doi.org/10.5897/AJAR2013.6931>

573 Pathare, P. B., Opara, U. L., Vigneault, C., Delele, M. A., & Al-Said, F. A. J. (2012). Design of packaging vents for
574 cooling fresh horticultural produce. *Food and Bioprocess Technology*, 5(6), 2031–2045.
575 <https://doi.org/10.1007/s11947-012-0883-9>

576 Robertson, G. L. (2016). *Food Packaging: Principles and Practice, Third Edition* (Third). Boca-Raton: Taylor &
577 Francis Group LLC. <https://doi.org/10.1177/0340035206070163>

578 Smale, N. J., Moureh, J., & Cortella, G. (2006). A review of numerical models of airflow in refrigerated food
579 applications. *International Journal of Refrigeration*, 29(6), 911–930.
580 <https://doi.org/10.1016/j.ijrefrig.2006.03.019>

581 Thompson. (2008). *Commercial cooling of fruits, vegetables and flowers*. University of California. California:
582 University of California.

583 Thompson, J. F. (2004). Pre-cooling and storage facilities. In USDA (Ed.), *USDA Agriculture Handbook Number*
584 *66: The Commercial Storage of Fruits, Vegetables, and Florist and Nursery Stocks* (pp. 1–10). USDA.
585 Retrieved from <http://www.ba.ars.usda.gov/hb66/contents.html>

586 Van Boekel, M. A. J. S. (2008). Kinetic modeling of food quality: A critical review. *Comprehensive Reviews in*
587 *Food Science and Food Safety*, 7, 144–158. <https://doi.org/10.1111/j.1541-4337.2007.00036.x>

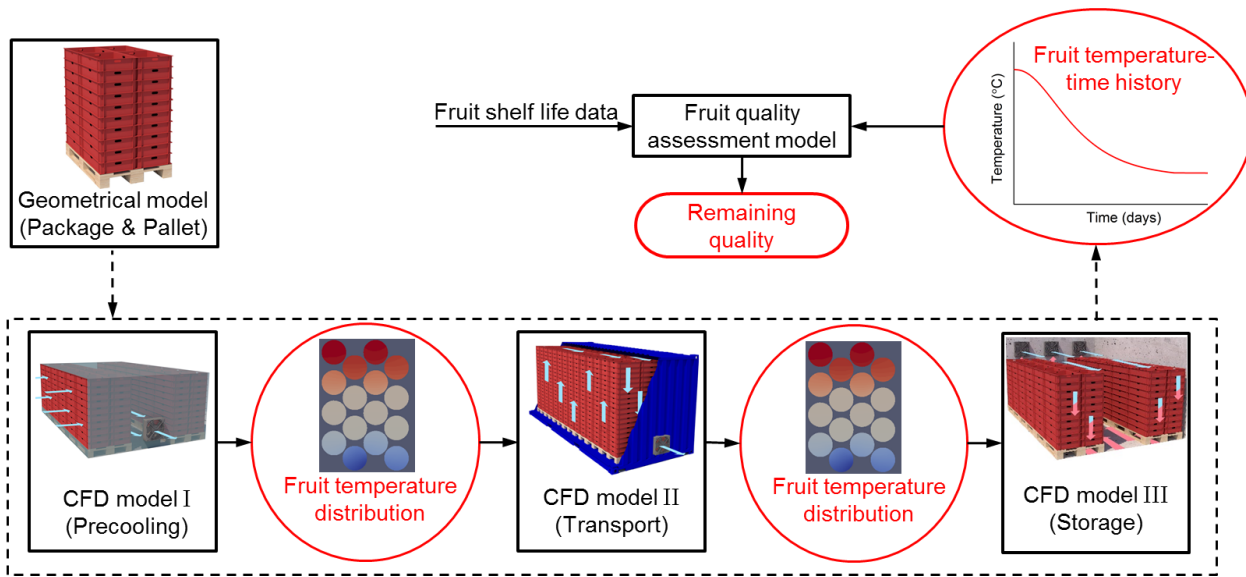
588 Vinyes, E., Asin, L., Alegre, S., Muñoz, P., Boschmonart, J., & Gasol, C. M. (2017). Life Cycle Assessment of
589 apple and peach production, distribution and consumption in Mediterranean fruit sector. *Journal of*
590 *Cleaner Production*, 149, 313–320. <https://doi.org/10.1016/j.jclepro.2017.02.102>

- 591 Wang, L., & Sun, D.-W. (2003). Recent developments in numerical modelling of heating and cooling processes
592 in the food industry—a review. *Trends in Food Science & Technology*, 14(10), 408–423.
593 [https://doi.org/10.1016/S0924-2244\(03\)00151-1](https://doi.org/10.1016/S0924-2244(03)00151-1)
- 594 Watkins, C. (2002). *Storage Technology for Apples and Pears. Postharvest Biology and Technology* (Vol. 24).
595 Victoria: Highway Press Pty Ltd. [https://doi.org/10.1016/S0925-5214\(01\)00140-5](https://doi.org/10.1016/S0925-5214(01)00140-5)
- 596 Wikström, F., Williams, H., Verghese, K., & Clune, S. (2014). The influence of packaging attributes on consumer
597 behaviour in food-packaging life cycle assessment studies - A neglected topic. *Journal of Cleaner*
598 *Production*, 73, 100–108. <https://doi.org/10.1016/j.jclepro.2013.10.042>
- 599 WPO. (2008). *World Packaging Organisation: Market statistics and future trends in global packaging*
600 *(www.worldpackaging.org)*. Retrieved from www.worldpackaging.org
- 601 Wu, W., Beretta, C., Cronje, P., Hellweg, S., & Defraeye, T. (2019). Integral performance evaluation of cold
602 chain scenarios and packaging of fresh fruit by combining virtual cold chains with environmental impact
603 assessment (in review). *Environmental Science & Technology*.
- 604 Wu, W., Häller, P., Cronje, P., & Defraeye, T. (2018). Full-scale experiments in forced-air precoolers with 40
605 pallets for citrus fruit: impact of packaging design and fruit size on cooling rate and heterogeneity.
606 *Biosystems Engineering*, 169, 115–125. <https://doi.org/10.1016/j.biosystemseng.2018.02.003>
- 607 Wu, Wentao, Cronjé, P., Nicolai, B., Verboven, P., Linus Opara, U., & Defraeye, T. (2018). Virtual cold chain
608 method to model the postharvest temperature history and quality evolution of fresh fruit – A case study
609 for citrus fruit packed in a single carton. *Computers and Electronics in Agriculture*, 144, 199–208.
610 <https://doi.org/10.1016/j.compag.2017.11.034>
- 611 Wu, Wentao, & Defraeye, T. (2018). Identifying heterogeneities in cooling and quality evolution for a pallet of

- 612 packed fresh fruit by using virtual cold chains. *Applied Thermal Engineering*, 133, 407–417.
- 613 <https://doi.org/10.1016/j.applthermaleng.2017.11.049>
- 614 Wu, Wentao, Yoon, N., Tong, Z., Chen, Y., Lv, Y., Aerenlund, T., & Benner, J. (2019). Diffuse ceiling ventilation
615 for buildings : A review of fundamental theories and research methodologies. *Journal of Cleaner
616 Production*, 211, 1600–1619. <https://doi.org/10.1016/j.jclepro.2018.11.148>
- 617 Xiao, X., Fu, Z., Zhu, Z., & Zhang, X. (2019). Improved preservation process for table grapes cleaner production
618 in cold chain. *Journal of Cleaner Production*, 211, 1171–1179.
619 <https://doi.org/10.1016/j.jclepro.2018.11.279>
- 620 Zhang, Q., Zhou, G., Qian, X., Yuan, M., Sun, Y., & Wang, D. (2018). Diffuse pollution characteristics of
621 respirable dust in fully-mechanized mining face under various velocities based on CFD investigation.
622 *Journal of Cleaner Production*, 184, 239–250. <https://doi.org/10.1016/j.jclepro.2018.02.230>

623

624



625

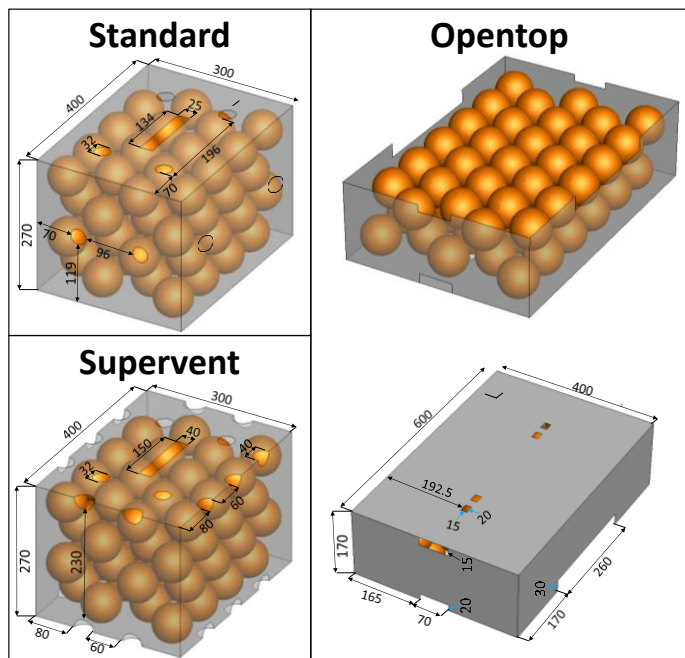
626

Figure 1. The Virtual Cold Chain (VCC) method illustrated by a typical cold chain consisting of precooling, refrigerated transport and cold storage (reproduced with permission from (Wentao Wu et al., 2018)).

627

628

629



630

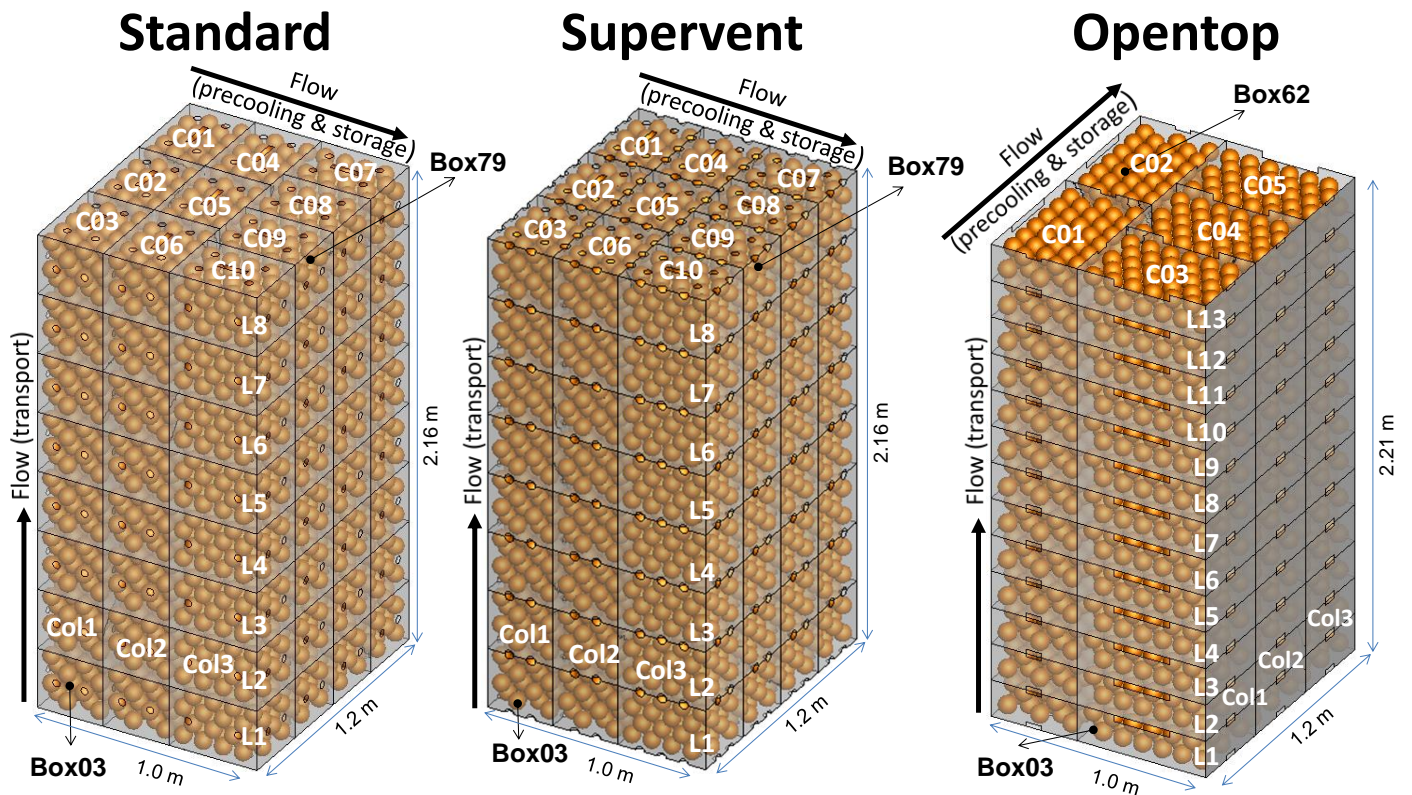
631

Figure 2. Geometry and dimensions of the Standard, Supervent and Opentop carton (view from the top and

632

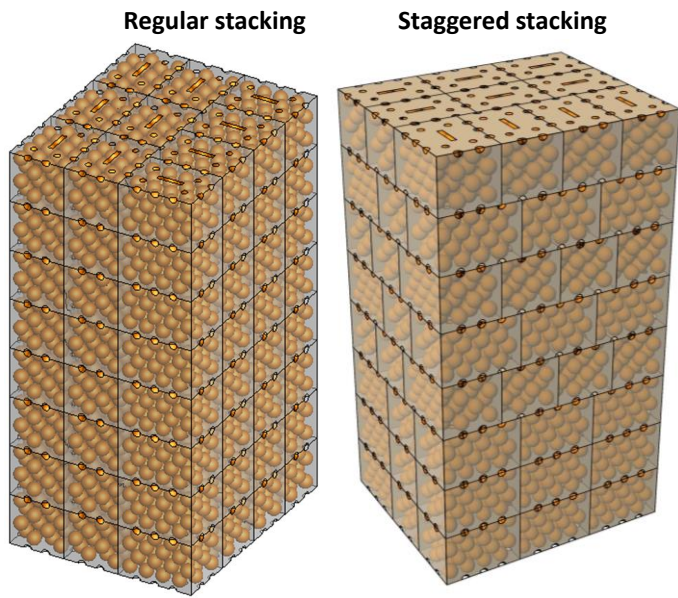
bottom), packed with orange fruit.

633



636 **Figure 3. High-cube citrus pallet of the Standard, Supervent and Opentop carton, stacked in different layers.**

638



639

640

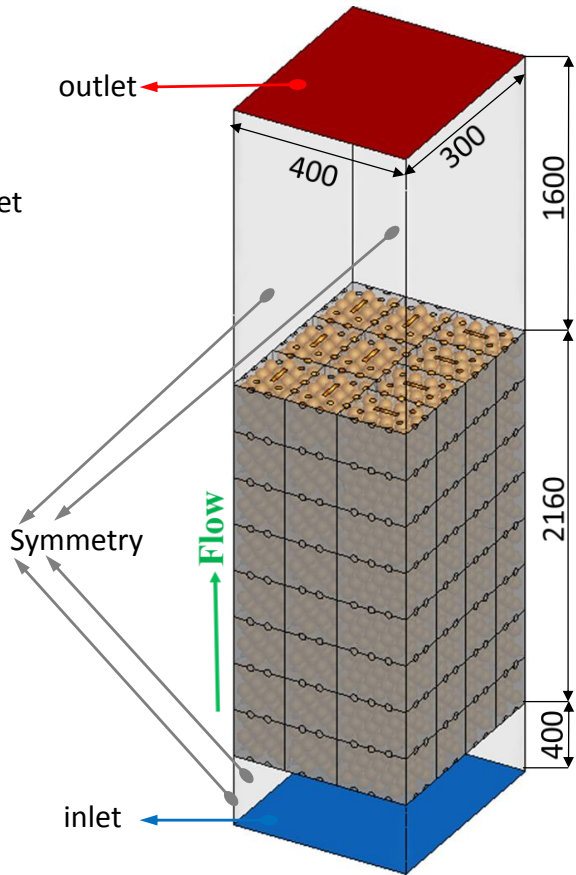
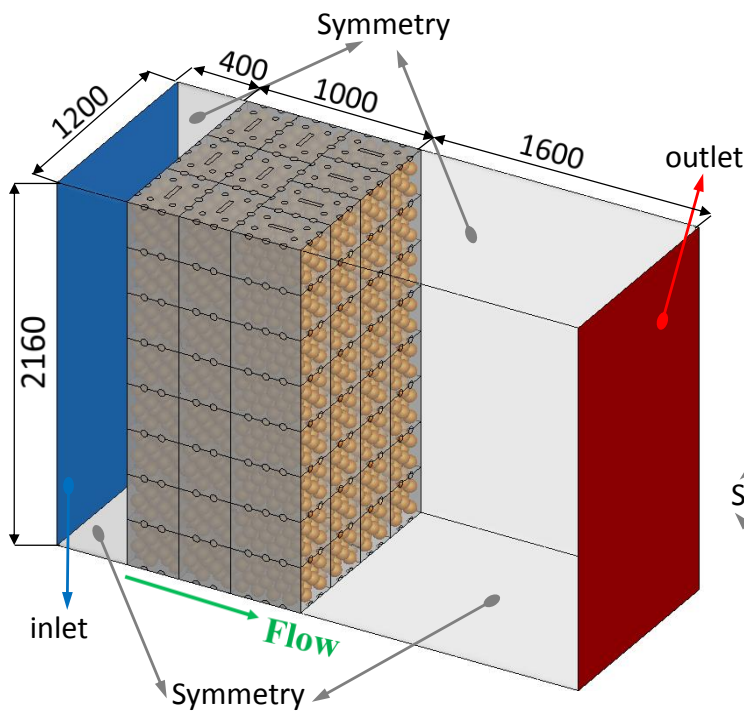
Figure 4. High-cube citrus pallet of the Supervent carton, according to a regular and a staggered stacking

641

pattern.

(a) Precooling and cold storage

(b) Refrigerated transport



642

643

644

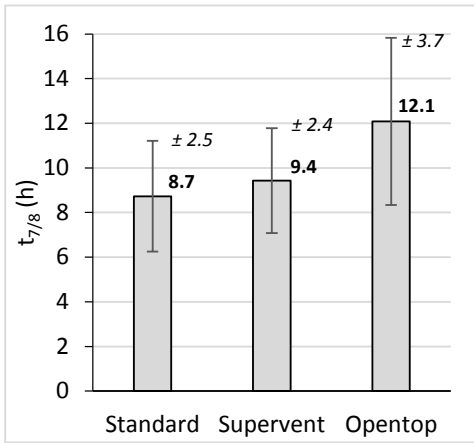
645

646

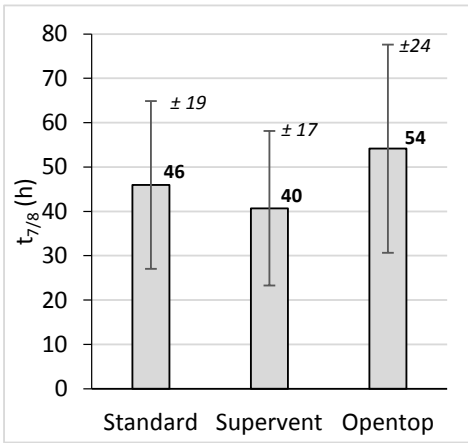
647

Figure 5. CFD models (with boundary conditions) for three unit operations, as illustrated for Supervent packaging: precooling, transport and refrigerated storage (units are in mm). Note that the pallet height is slightly different for Opentop packaging.

(a) Precooling



(b) Transport



(c) Storage

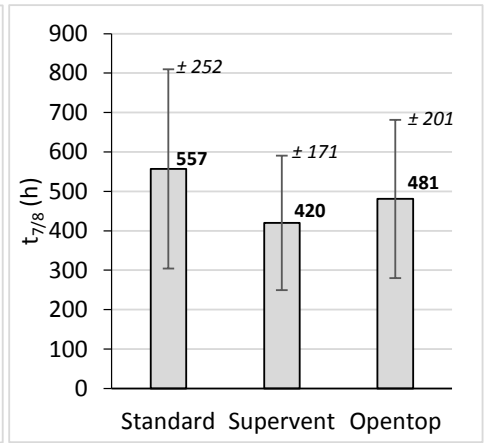
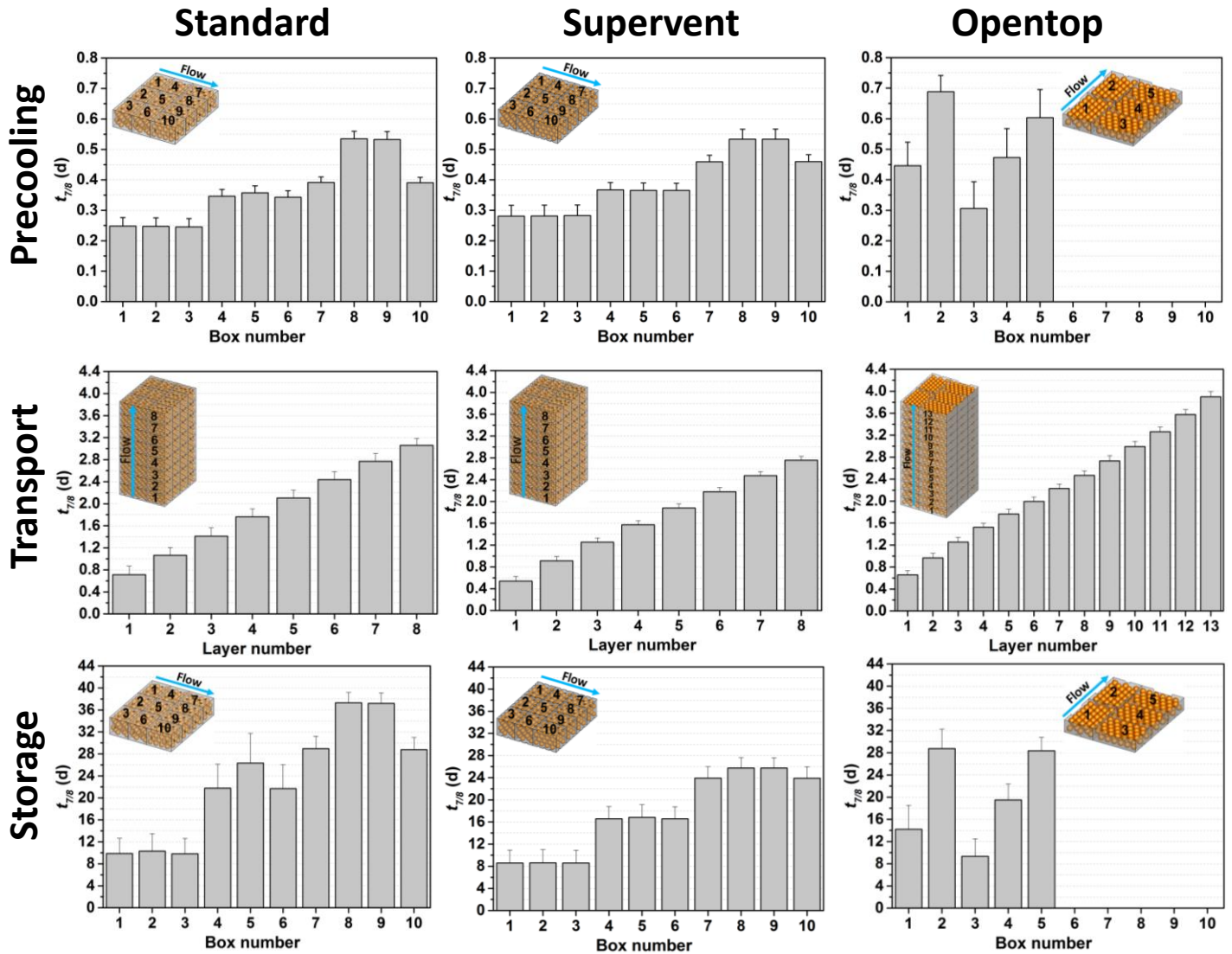


Figure 6. Seven-eighths cooling time of the fruit during precooling, refrigerated transport and refrigerated storage for three packaging: SECT averaged over an entire pallet of fruit and the standard deviation.



652

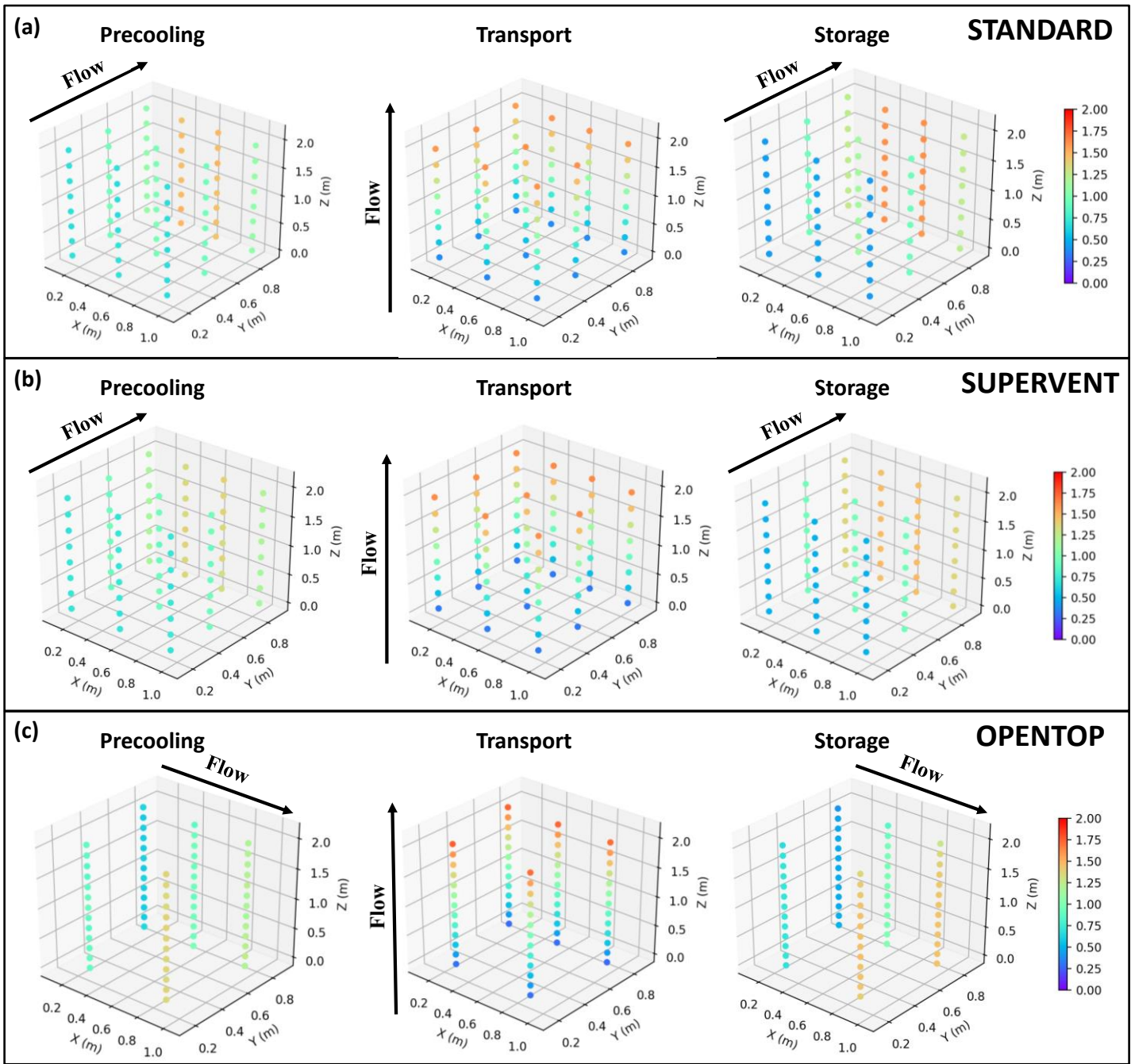
653

654

655

656

Figure 7. Seven-eighths cooling time ($t_{7/8}$) for each single box (C01-C10) for precooling and storage (averaged over all boxes in each vertical column and corresponding standard deviation), and for each horizontal layer of boxes (L1-L13) for transport (averaged value over all boxes in each layer and corresponding standard deviation).



657

658

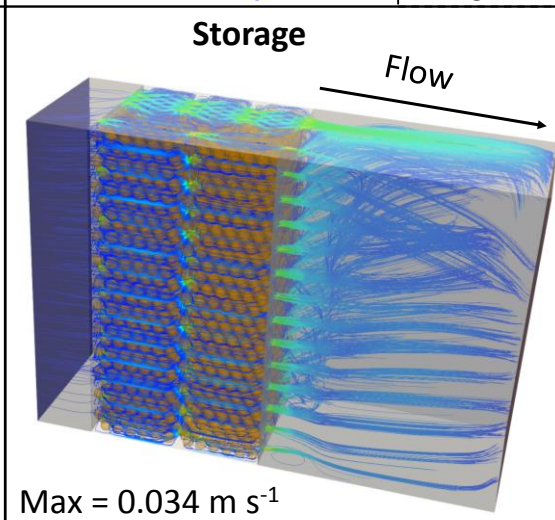
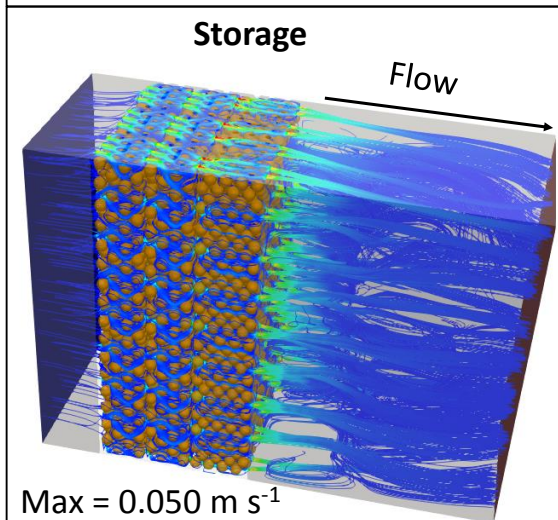
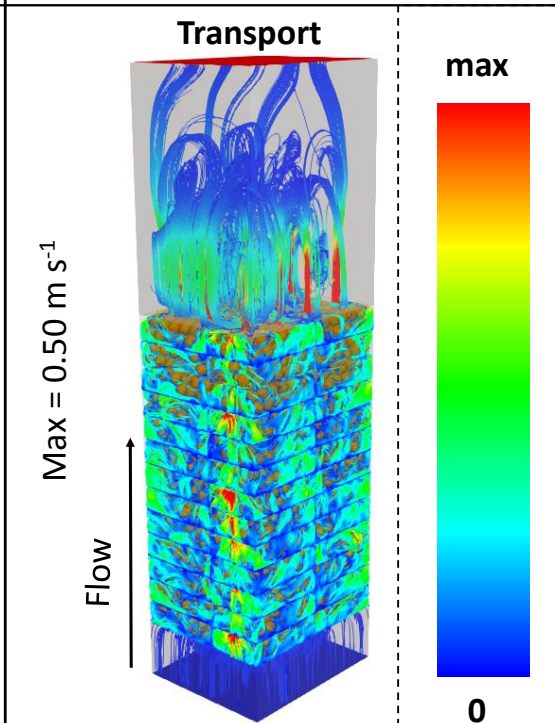
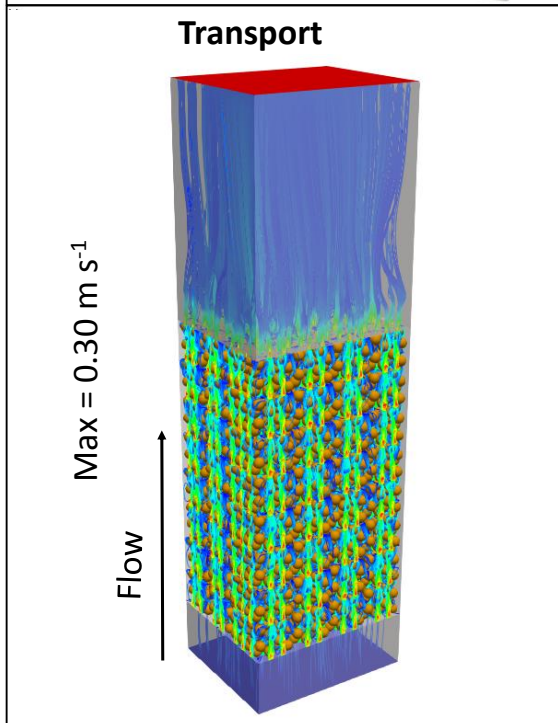
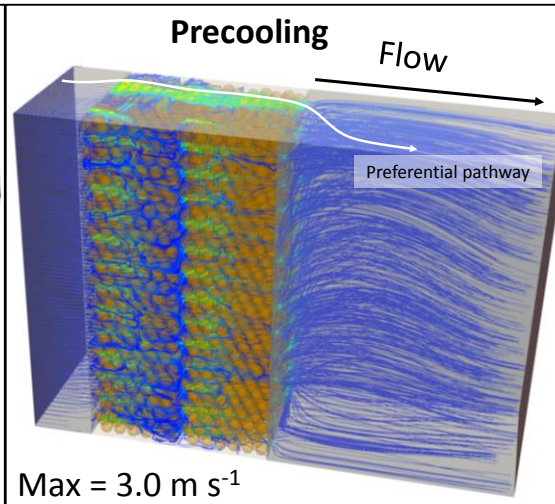
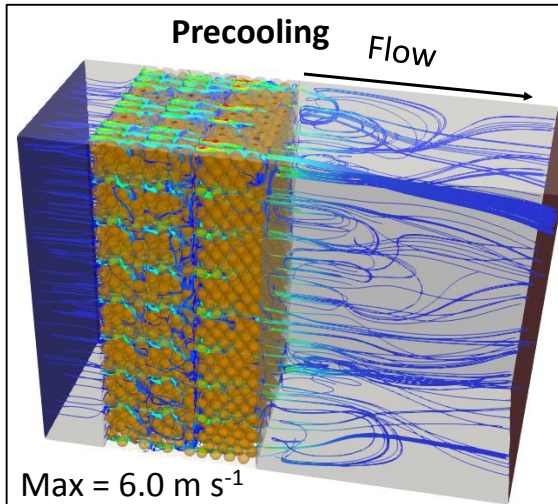
659

660

Figure 8. Seven-eighths cooling time for a pallet of Standard, Supervent and Opentop packaging for three unit operations (scaled with the average SECT for that pallet for that unit operation, namely $SECT_{avg}$), where each colored dot represents the averaged value of the $SECT/SECT_{avg}$ over a single box.

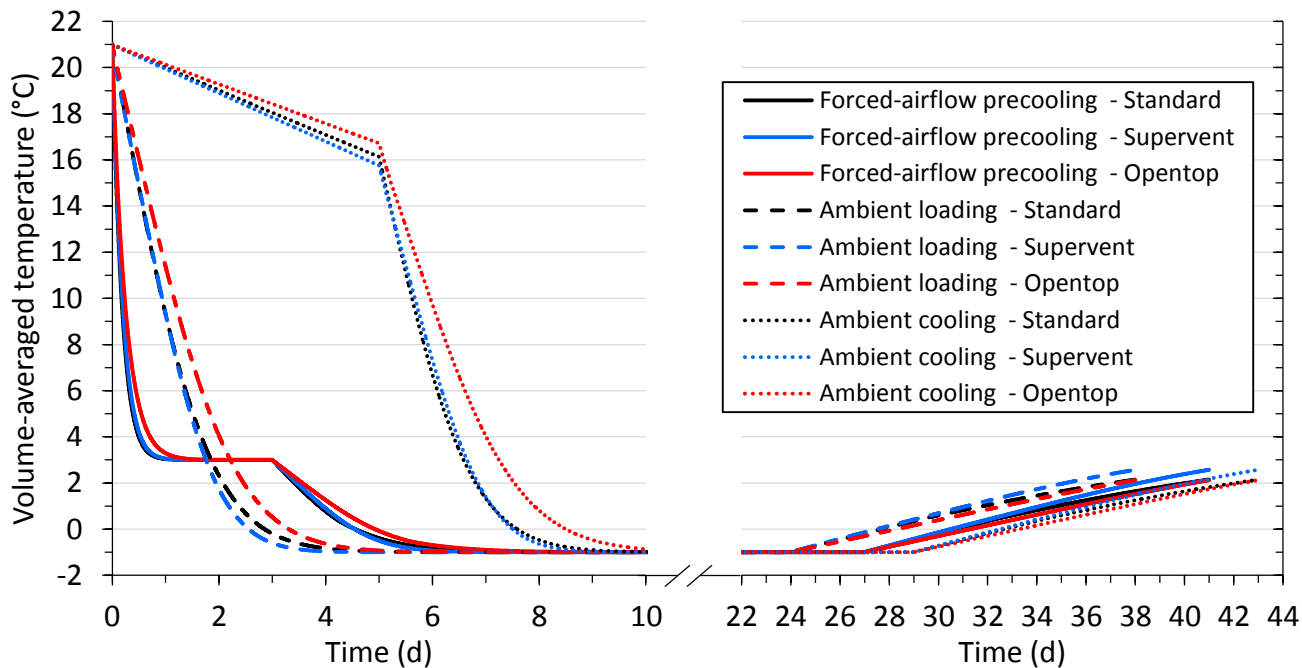
(a) SUPERVENT

(b) OPENTOP



662 **Figure 9. Streamlines for a pallet of Supervent and Opentop packaging for three unit operations. The color**
663 **bar is valid for each graph and the maximal values are indicated separately.**

664

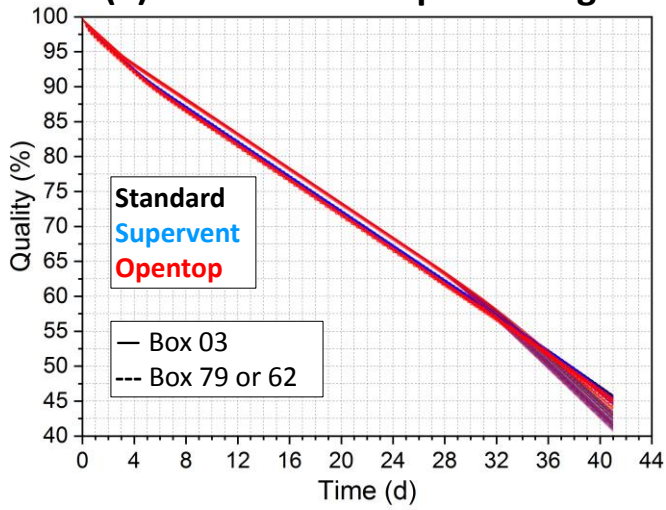


665

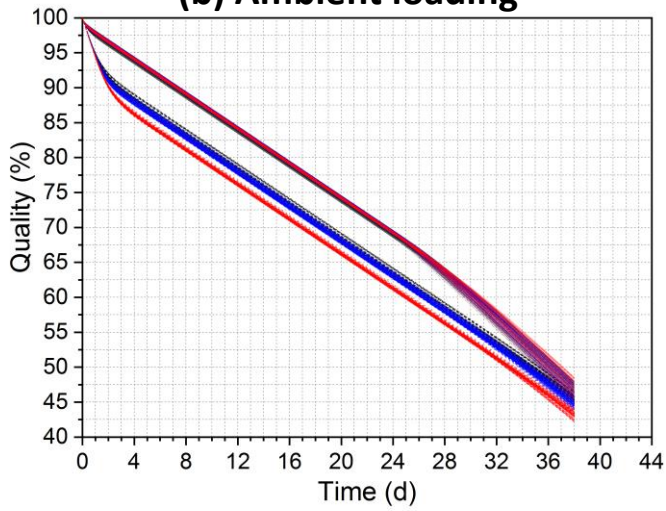
666 **Figure 10. Volume-averaged temperature over all fruit in a pallet as a function of time in the three cold**
667 **chain scenarios for all packaging designs.**

668

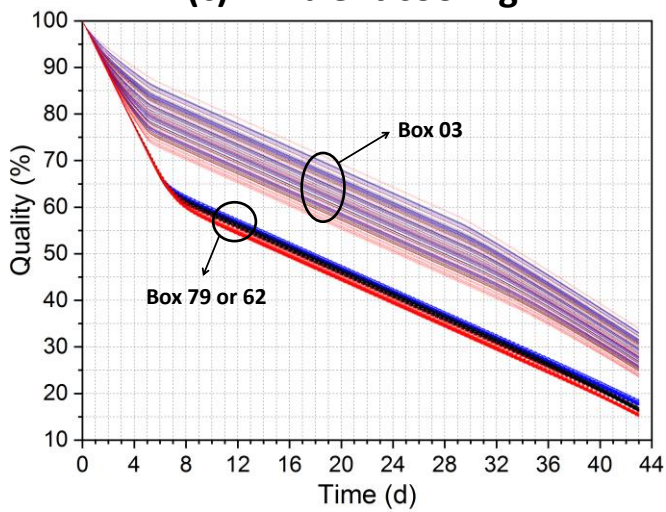
(a) Forced-airflow precooling



(b) Ambient loading



(c) Ambient cooling



670 **Figure 11. Quality evolution of individual fruit in Box03 and Box79 on a pallet with Standard (black lines) or**
671 **Supervent (blue lines) cartons, and in Box03 and Box62 on a pallet with Opentop cartons (red lines) for the**
672 **(a) forced-airflow cooling chain, (b) ambient loading chain, (c) ambient cooling chain.**

673

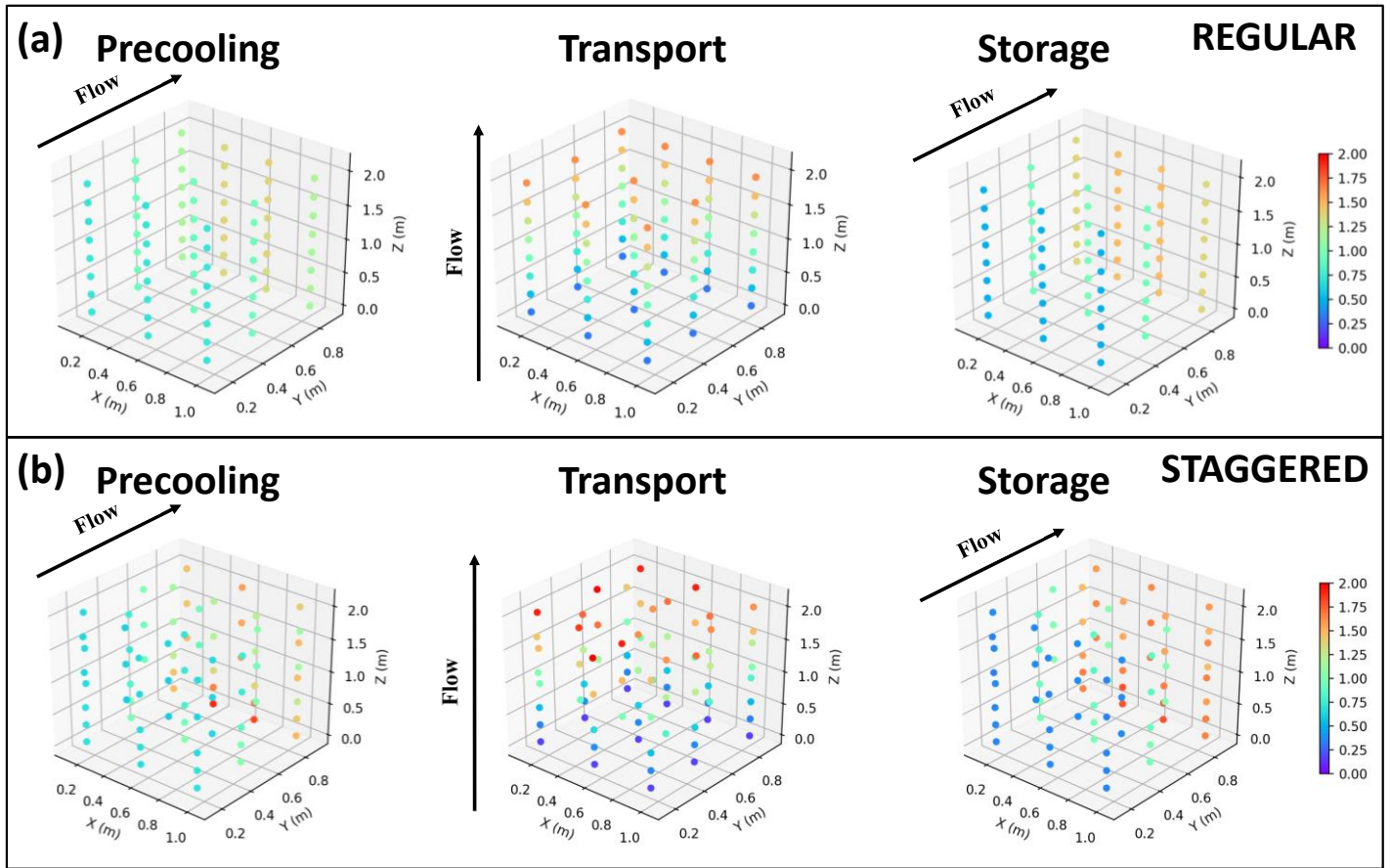


Figure 12. Seven-eighths cooling time for a pallet of Supervent packaging for three unit operations (scaled with the average SECT for that pallet for that unit operation, namely $SECT_{avg}$), for two different pallet stacking configurations (Figure 4): regular (results reported also in Figure 8) and staggered. Each colored dot represents the averaged value of the $SECT/SECT_{avg}$ over a single box.

681

682 **Table 1. Total open area of the ventilation openings along the surfaces of each carton.**

	Standard	Supervent	Opentop
Long side	1.5%	3.5%	7.6%
Short side	2.0%	3.1%	3.6%
Bottom	5.5%	10.7%	0.5%

683

684

685

686 **Table 2. Boundary conditions for the different cold chain scenarios (a dash means that the cold chain does**
 687 **not contain the corresponding unit operation.).**

688

Cold chain scenario	Precooling	Cold storage before shipment	Cold storage after shipment	Cold storage after shipment
Forced-airflow precooling	0.2 L kg ⁻¹ s ⁻¹ 3 °C 3 days	-	0.02 L kg ⁻¹ s ⁻¹ -1 °C 24 days	0.002 L kg ⁻¹ s ⁻¹ 4 °C 14 days
Ambient cooling	-	0.002 L kg ⁻¹ s ⁻¹ 3 °C 5 days	0.02 L kg ⁻¹ s ⁻¹ -1 °C 24 days	0.002 L kg ⁻¹ s ⁻¹ 4 °C 14 days
Ambient loading	-	-	0.02 L kg ⁻¹ s ⁻¹ -1 °C 24 days	0.002 L kg ⁻¹ s ⁻¹ 4 °C 14 days

689

690

691

692